

A Hard X-ray View of Accreting X-ray Binary Pulsars

MAURO ORLANDINI

Istituto di Astrofisica Spaziale e Fisica Cosmica (IASF/CNR) — Sezione di Bologna

ABSTRACT. The study of the hard ($E \gtrsim 10$ keV) energy spectra of X-ray binary pulsars can give a wealth of information on the physical processes that occur close to the neutron star surface. Extreme matter regimes are probed, and precious information on how matter and radiation behave and interact in critical conditions can be obtained. We will give an overview on the most recent results obtained by RXTE and BeppoSAX on this class of objects, in order to pass the baton onto just launched experiments, like INTEGRAL, or soon to be launched, like AGILE and ASTRO-E2.

1. Introduction

The discovery of X-ray emission from celestial objects further extended the knowledge of our Universe, which resulted very different from the quiet and calm Universe the astronomers of the last centuries described. Indeed, it was just at the beginning of the 1960's that, with the advent of stratospheric balloons and rockets, it was possible to launch outside our atmosphere some Geiger counters (Giacconi et al. 1962). In this way, the first discrete X-ray source in our Galaxy was discovered: Sco X-1. In 1966 the first optical counterpart to a galactic X-ray source, Sco X-1, was identified with an old 12th–13th magnitude star (Sandage et al. 1966). In the following years a theoretical model was developed according to which galactic X-ray sources are close, interacting binary systems composed by a “normal” star and a compact object (Shklovskii 1967). In the same years it was understood that spherical accretion could become non symmetric, leading to the formation of an accretion disk around the compact object, if the accreting matter possesses enough angular momentum (Prendergast & Burbidge 1968).

But the decisive step toward the comprehension of this class of objects was achieved with the discovery of pulsed emission from some X-ray sources (Giacconi et al. 1971; Tananbaum et al. 1972). Indeed, the variability on short time scale — for example the first discovered X-ray binary pulsar, Cen X-3, spins at about 4.8 s — implies a small emitting region. Furthermore, because the system is not destroyed by the centrifugal force it is necessary that at the surface of the emitting object the gravitational force is greater than the centrifugal one. This implies $\Omega_p \gtrsim \sqrt{G\langle\rho\rangle}$, where Ω_p is the spin frequency, G the gravitational constant and $\langle\rho\rangle$ the object mean density. The observed values of Ω_p imply $\langle\rho\rangle \gtrsim 10^6$ g/cm³, and therefore the compact nature of the object responsible of the pulsed X-ray emission was established. The only compact object able to explain all the phenomena observed in X-ray pulsars, as pulse period range and surface magnetic field strength, is a neutron star (see, e.g., Shapiro & Teukolsky 1983).

The standard model explains the X-ray emission as due to the conversion of the kinetic energy of the in-falling matter (coming from the intense stellar wind of an early optical star, in this case we speak about wind-fed binaries, or from an accretion disk due to Roche-lobe overflow, and this is the case of disk-fed binaries) into radiation, because of the interactions with the strong magnetic field of the neutron star, of the order of 10^{11} – 10^{13} G¹. The dipolar magnetic field of the compact object drives the accreted matter onto the magnetic polar caps, and if the magnetic field axis is not aligned with the spin

¹ Obtained from conservation of magnetic flux during the process of collapse from a “normal” star ($B \sim 10$ – 100 G, $R \sim 10^6$ Km) to a neutron star ($R \sim 10$ Km) and lately confirmed by the observation of cyclotron resonance features (see below).

axis then the compact object acts as a “lighthouse”, giving rise to pulsed emission when the beam (or the beams, according to the geometry) crosses our line of sight.

Subsequent observations clearly demonstrated the binary nature of these objects by observations of X-ray eclipses and Doppler delays in the pulse arrival times (Schreier et al. 1972). From these measurements it was possible to “solve” the binary systems, obtaining masses in agreement with that expected for a neutron star. But for some X-ray pulsars, with pulse periods in the 5–12 s range, every attempt to find signatures of binary motion was unsuccessful. It was later recognized that they form a class of their own, the so-called anomalous X-ray pulsars, in which their X-ray emission is due to the conversion of the magnetic field energy into radiation (Thompson & Duncan 1995; 1996). We will not discuss here on this quite interesting class (see, e.g., Mereghetti et al. 2002 for a review).

2. Astrophysics of X-ray binary pulsars

The main astrophysical problem connected with the physics of X-ray pulsars is that we cannot use a linearized theory but we are forced to use the full magneto-hydrodynamical one. This is due to the fact that the coupling constants of the interactions (in this case gravitational and magnetic) are so large that a series expansion is not possible. Furthermore, the highly non-linear nature of the problem makes its treatment very difficult. In Fig. 1 a sort of block diagram of the physical processes of production and emission of the X-ray flux in a X-ray binary pulsar is shown.

Each block in Fig. 1 is characterized by its typical physical processes and characteristic time and length scales. In the first block we deal with the problem of determining how much matter is captured by the neutron star gravitational field and how its angular momentum is transferred to the neutron star (this will have important consequences on the spinning behavior of the neutron star). All the matter swept by the neutron star inside a distance called “accretion radius” will be captured and accreted. This radius depends on the relative velocity of the wind matter with respect to the neutron star (Bondi & Hoyle 1944):

$$r_a = \frac{2GM_x}{v_{\text{rel}}^2 + c_s^2} \approx \frac{2GM_x}{v_{\text{orb}}^2 + v_{\text{win}}^2} \quad (1)$$

where M_x is the neutron star mass, c_s is the sound speed (negligible because the wind matter is supersonic; Elsner & Lamb 1977), and v_{orb} and v_{win} are the orbital and wind velocity, respectively. We expect that the characteristic time scales in this “block” be dynamical, of the order of 100–1000 s.

It is worthy to introduce here another scale length, connected to the rotation of the neutron star. In order for matter to be accreted it is necessary that the neutron star does not rotate so fast that plasma is expelled because of the centrifugal force. The distance at which there is balance between these two forces is called corotation radius, defined as

$$r_c = \left(\frac{GM_x}{\Omega_p^2} \right)^{1/3} = 1.5 \times 10^8 P^{2/3} m^{1/3} \text{ cm} \quad (2)$$

where P is the pulse period in seconds, and m the neutron star mass in solar units.

At some distance from the neutron star surface, called magnetospheric radius, the magnetic field of the neutron star becomes the main interaction which drives the motion of the captured matter toward the stellar surface. At this distance matter is halted by the very strong magnetic field of the neutron star and accretion can occur only if matter can penetrate the shock layer by means of magneto-hydrodynamical instabilities (Elsner & Lamb 1977). From its definition, the magnetospheric radius will depend on the magnetic

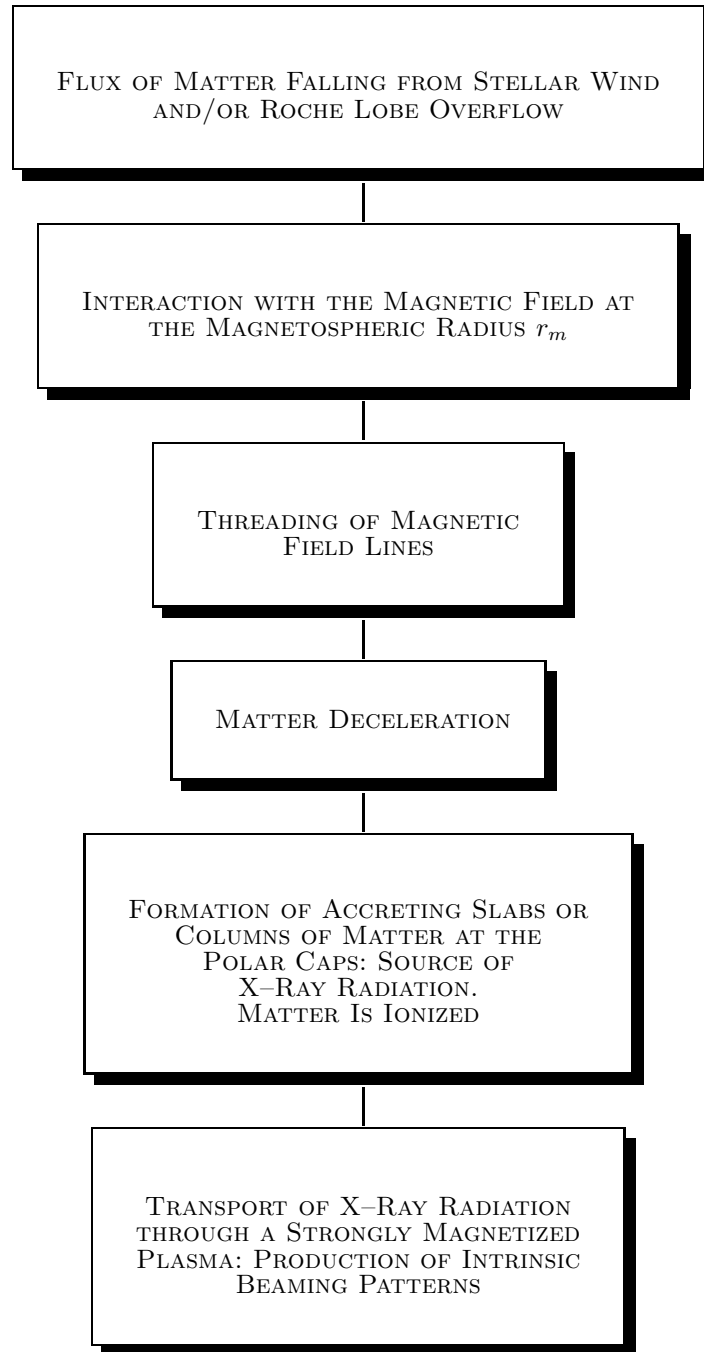


Fig. 1. Block diagram of the physical processes of production and emission of the X-ray flux in a X-ray binary pulsar.

field strength and the ram pressure of the accreted matter (see, e.g., Frank, King & Raine 1985):

$$r_m = \begin{cases} 5.1 \times 10^8 \xi^{2/7} \mu_{30}^{4/7} m^{-1/7} \dot{M}_{16}^{-2/7} \text{ cm} \\ 2.9 \times 10^8 \xi^{2/7} \mu_{30}^{4/7} m^{-1/7} r_6^{-2/7} \epsilon_{0.1}^{2/7} L_{37}^{-2/7} \text{ cm} \end{cases} \quad (3)$$

where $\xi \lesssim 1$, μ_{30} is the dipolar magnetic moment in units of 10^{30} G cm³, \dot{M}_{16} the mass accretion rate onto the neutron star in units of 10^{16} g/s, r_6 the neutron star radius in units of 10^6 cm, $\epsilon_{0.1}$ the accretion efficiency in units of 0.1, and L_{37} the X-ray luminosity in units of 10^{37} erg/s. Because the main physical processes occurring in this “block” are magneto-hydrodynamical instabilities, the characteristic time scales will be 0.1–10 s.

According to fastness of rotation, different kind of instabilities will determine plasma penetration (Arons & Lea 1976): in the case of slow rotators² plasma penetration will occur mainly by means of gravity-driven interchange (Rayleigh-Taylor) instability. Decreasing the pulse period, the shear between the plasma and the magnetosphere becomes more and more important, leading to the stabilization of the magnetopause with respect to Rayleigh-Taylor instability, and giving rise to the onset of Kelvin-Helmholtz instability.

By comparing the two length scales, magnetospheric and corotation radii, it is possible to distinguish two accretion regimes: if $r_c \gtrsim r_m$ then at the magnetospheric limit, when plasma penetrates the magnetosphere, the centrifugal force is smaller than the magnetic force, and therefore matter can be accreted. This is the so-called *accretor* regime. On the other hand, if $r_c \lesssim r_m$ then the centrifugal force inhibits matter from being channeled and is swept away. This is the so-called *propeller* regime (Illarionov & Sunyaev 1975).

Once matter has penetrated the magnetosphere, it will follow the magnetic field lines up to the magnetic polar caps of the neutron star, where it will be decelerated. If the amount of matter falling on the polar caps is high enough that a X-ray luminosity greater than about 10^{37} erg/s is reached, then a radiative shock will form (Basko & Sunyaev 1976). In this case an accretion column just above the polar cap will form; this accretion column will be optically thick to X-rays, therefore radiation will be emitted mainly *sideways*. Radiation is emitted mainly in a direction perpendicular to the magnetic field lines and we call this pattern “fan beam emission pattern”.

On the other hand, if the X-ray luminosity is lower than about 10^{37} erg/s, then the radiative shock will not form and matter will be able to reach the neutron star surface. In this case we will have the formation of an emitting “slab” and radiation will be emitted mainly in a direction parallel to the magnetic field lines. We call this pattern “pencil beam emission pattern”. Because the main physical processes occurring in this “box” are Compton heating and cooling, bremsstrahlung and Coulomb interactions, the characteristic time scale will be $\lesssim 0.001$ s.

Before leaving the neutron star, radiation interacts with the surrounding medium and the very strong magnetic field. As briefly discussed above, this interaction is very difficult to treat because of the impossibility to linearize the theory due to our substantial ignorance on very strong magnetic fields (see Harding 2003 for a recent review). One of the most important consequences of the presence of a strong magnetic field is the quantization of the electron motion in the direction transverse to B : this leads to the so-called Landau levels (see Mészáros 1992 for a complete treatment of this topic). In the non-relativistic case, the energy associated to each level is given by

² Slow rotators have pulse frequency so small that rotation can be neglected in all the equations describing the physics of accretion. A quantitative parameter which measures the importance of rotation is the “fastness parameter”, defined as (Elsner & Lamb 1977): $\omega_k \equiv \Omega_p / \Omega_k(r_m)$, where Ω_k is the angular velocity of matter orbiting into Keplerian orbits. If $\omega_k \ll 1$ rotation can be neglected.

$$\hbar\omega_n = n \hbar\omega_c \quad (4)$$

where the Larmor gyro-frequency ω_c is defined as $eB/\gamma mc$, with γ the Lorentz factor, e and mc the electron charge and momentum, respectively. As an aside, from Eq. 4 we have that $E_n = 11.6 \cdot B_{12}$ keV, where B_{12} is the magnetic field strength in units of 10^{12} G, and therefore observable in the hard X-ray energy band. When relativistic corrections are taken into account a slight non-harmonicity is introduced in the Landau levels. Indeed, we have

$$\hbar\omega_n = mc^2 \frac{\sqrt{mc^2 + 2n\hbar\omega_c \sin^2\theta} - 1}{\sin^2\theta} \quad (5)$$

where θ is the angle between the line of sight and B .

Due to the existence of these levels, an electromagnetic wave which propagates in such a plasma will have well defined polarization normal modes, *i.e.* the medium will be birefringent (Ginzburg 1970). Furthermore, for magnetic fields not far from the critical value of $1.414 \cdot 10^{13}$ G, an important rôle is played by virtual electron-positron pairs. The corresponding virtual photons dominate the polarization properties of the medium and therefore the radiative opacity of the plasma. This means that the scattering cross sections of X-rays are strongly anisotropic and energy dependent (Herold 1979).

It is important to stress that the cyclotron *absorption* cross section is resonant for energies equal to the gyro-magnetic (Larmor) frequency ω_c . Once the electron absorbs a photon it (almost) immediately de-excites on a time scale $t_r \sim 2.6 \times 10^{-16} B_{12}^{-1}$ sec (Mészáros 1992). This has important consequences for the *scattering* cross sections. Indeed, while a scattering process involves two photons (one going in, one going out), absorption (or emission) processes involve only one photon. Therefore one expects that the two cross sections are different. This is not true just because an absorbed photon is immediately re-emitted, and therefore the absorption-emission process is equivalent to a scattering. Therefore photons with frequency close to ω_c will be scattered out of the line of sight, creating a drop in their number. Cyclotron “lines” observed in the spectra of X-ray binary pulsars are therefore *not* due to absorption processes, but are due to scattering of photons resonant with the magnetospheric electrons (as it occurs for the Fraunhofer lines in the Solar spectrum). This is why we will not use the term cyclotron lines but the more appropriate “cyclotron resonant features” (CRFs).

3. Observation of X-ray binary pulsars

As we pointed out in the previous section, a great deal of information can be obtained by the observation of the hard ($E \gtrsim 10$ keV) spectra of X-ray binary pulsars. The advantage of focusing on the hard X-rays is that in this energy range we are observing phenomena that occur close to the neutron star surface and that are less subject to absorption phenomena that alter the emergent spectra. An overview of past hard X-ray observations is already available in literature (see e.g. Orlandini & Dal Fiume 2001) therefore we will focus on recent results that can be used as starting point for present and future missions, like INTEGRAL, AGILE and ASTRO-E2.

The best recent X-ray telescopes suited for the study of X-ray binaries are (or have been) RXTE and BeppoSAX (in particular the two high energy instruments HEXTE and PDS). The advantage of BeppoSAX with respect to its US fellow was its larger band-pass, fundamental for the reconstruction of the continuum, and the lower intrinsic background that allowed a better sensitivity. Anyway, both satellites gave a wealth of new information and opened a new era for the study of X-ray pulsars, passing the baton onto the just launched INTEGRAL.

In Table I we list the X-ray binary pulsars observed by BeppoSAX and about which we will discuss in this paper (for a complete discussion on the RXTE observations of

TABLE I
BeppoSAX observations of X-ray binary pulsars

Source	Obs Date	E_{cyc} (keV)	FWHM (keV)	References
4U0115+63 (M)	20 Mar 1999	12.78 ± 0.08	3.58 ± 0.33	Santangelo et al. 1999
4U1538-52 (M)	29 Jul 1998	21.5 ± 0.4	6.7 ± 1.2	Robba et al. 2001
<u>Cen X-3 (M?)</u>	27 Feb 1997	28.5 ± 0.5	7.3 ± 1.9	Santangelo et al. 1998
<u>XTE J1946+27</u>	09 Oct 1998	33 ± 4	16 ± 2	Orlandini et al. 2001
<u>OA01657-415</u>	04 Sep 1998	36 ± 2	10	Orlandini et al. 1999
<u>4U1626-67</u>	06 Aug 1996	38.0 ± 0.9	11.8 ± 1.7	Orlandini et al. 1998b
4U1907+09 (M)	29 Sep 1997	38.3 ± 0.7	9.7 ± 2.3	Cusumano et al. 1998
Her X-1	27 Jul 1996	42.1 ± 0.3	14.7 ± 1.1	Dal Fiume et al. 1998
<u>GX301-2</u>	24 Jan 1998	49.5 ± 1.0	17.9 ± 2.5	Orlandini et al. 2000
<u>Vela X-1</u>	14 Jul 1996	54.8 ± 0.9	25.0 ± 2.1	Orlandini et al. 1998a
A0535+26	04 Sep 2000	118 ± 20	81 ± 50	Orlandini et al. 2004
GX1+4	25 Mar 1997	Israel et al. 1998
GS1843+00	04 Apr 1997	Piraino et al. 2000
X Persei	09 Sep 1996	Di Salvo et al. 1998

Sources underlined are discoveries made by BeppoSAX — M stands for multiple lines detected/suspected

X-ray pulsars see Coburn et al. 2002). For each of them we present the value of its CRF energy, if observed.

3.1. The X-ray continuum

The characterization of the continuum is of paramount importance for the determination of the physical processes that are at play. As it should be clear from the Introduction, the main physical process responsible for the continuum emission in X-ray binary pulsars is Compton scattering. Broadly speaking, there are two regimes as a function of the comptonization parameter y , that give rise to two completely different emergent spectra. If $y \ll 1$ only coherent scattering will be important, and the emergent spectrum will be a blackbody spectrum or a “modified” blackbody spectrum according whether the photon frequency is lower or greater than the frequency at which scattering and absorption coefficients are equal (Rybicki & Lightman 1975).

On the other hand, if $y \gg 1$ then inverse Compton scattering can be important. If we define a frequency ω_{co} such that $y(\omega_{co}) = 1$, then for $\omega \gg \omega_{co}$ the inverse Compton scattering is saturated and the emergent spectrum will show a Wien hump, due to low-energy photons up-scattered up to $\hbar\omega \sim 3kT$ (Rybicki & Lightman 1975). In the case in which there is not saturation a detailed analysis of the Kompaneets equation shows that the spectrum will have the form of a power law modified by a high energy cutoff

(Rybicki & Lightman 1975; Sunyaev & Titarchuk 1980).

On the observational point of view, the first attempt to describe X-ray pulsar spectra was done by White et al. (1983) who introduced a cutoff power law that mimicked the unsaturated inverse Compton process. In order to “smooth” the break around the cutoff energy, Tanaka (1986) introduced the so-called Fermi-Dirac cutoff, but there was no physical meaning for the fitting parameters. The discovery of a correlation between the cutoff energy and the CRF energy by Makishima and Mihara (1992) led Mihara (1995) to introduce the first analytical fitting law with a clear physical meaning of its parameters, the so-called NPEX (Negative Positive Exponential) model:

$$\text{NPEX}(E) = (AE^{-\alpha} + BE^{+\beta}) \exp\left(-\frac{E}{kT}\right) . \quad (6)$$

This model is quite successful in describing the X-ray pulsar spectra observed by Ginga in the 3–30 keV. Its components have also a physical meaning, because it mimics the saturated inverse Compton spectrum. Furthermore, because the (non relativistic) energy variation of a photon during Compton scattering is $\Delta E/E = (4kT - E)/mc^2$ (Rybicki & Lightman 1975) then when $E = E_c$ the medium is optically thick and therefore $E_c \sim 4kT$.

From an observational point of view, the X-ray pulsars observed by BeppoSAX and listed in Table I cannot be well fit by Eq. 6. In particular, we find that their continuum can be described in terms of (i) a black-body component with temperature of few hundreds eV; (ii) a power law of photon index ~ 1 up to ~ 10 keV; and a (iii) a high energy ($\gtrsim 10$ keV) cutoff that makes the spectrum rapidly drop above ~ 40 – 50 keV.

Particular care must be taken in the description of the cutoff. Indeed, an incorrect parametrization of the change of slope can introduce features that are not real but dependent on the choice of the functional adopted to model the continuum. In particular, for the X-ray pulsar OAO1657–415 it was clearly detected a two-step steepening of the spectrum (Orlandini et al. 1999): a first change of slope occurring in the ~ 10 – 20 keV range, while a second steepening occurring at higher energies. By using a single-step steepening model will give as a result the creation of features that could be erroneously attributed to CRFs. We think this is the case for the claimed CRF at ~ 25 keV in Vela X–1 (Orlandini et al. 1998a; Kreykenbohm et al. 2002). Indeed, by using a smoother description of the cutoff, La Barbera et al. (2003) showed that the ~ 25 keV CRF is not necessary for fitting the Vela X–1 spectra.

Another possible source of confusion could be raised by features due instrumental effects. A standard way to remove these effects is to normalize the source observed spectrum, channel by channel, to the Crab spectrum. The Crab nebula is considered a “standard candle” in X-ray astronomy, because of its brightness, steadiness, and featureless single power law spectrum. If a feature is instrumental, then it should be washed out in the Crab ratio. As we will show in the next section, we will use this tool to clearly identify features in the spectra of X-ray pulsars.

3.2. Cyclotron resonance features

The very first observation of a CRF in a spectrum of an X-ray pulsar was performed in 1978 when Trümper et al. observed a ~ 35 keV CRF in the spectrum of Her X–1. A while later, in the spectrum of the transient X-ray pulsar 4U0115+63 not only the fundamental but also the first harmonics was observed (Wheaton et al. 1979). Observations of CRFs in other X-ray pulsars showed that they are a quite common phenomenon in this class of objects. At the beginning they were described empirically as an *additive* Gaussian in absorption (*i.e.* a Gaussian function with negative normalization). Because CRFs are broad features, this modeling did not fit well because it depends on the adopted contin-

uum, therefore Soong et al. (1990) introduced the *multiplicative* Gaussian in absorption, defined as

$$\text{GAUABS}(E) = \left[1 - I \exp \left(-\frac{(E - E_c)^2}{2W^2} \right) \right] . \quad (7)$$

Mihara (1995), on the other hand, introduced a different description of the CRF in terms on a Lorentzian function, led by the fact that the cyclotron scattering cross section has this form. The so-called cyclotron absorption function has the form

$$\text{CYAB}(E) = \exp \left(-\frac{\tau(W E/E_c)^2}{(E - E_c)^2 + W^2} \right) . \quad (8)$$

The BeppoSAX observations showed us that Eq. 7 is a better description of CRFs: the reason is that Eq. 8 is deeply connected with the NPEX continuum. Indeed, the CYAB description of the CRF should be used *only* together with the NPEX continuum. We observed that the inclusion of Eq. 8 on a power law continuum results in changing the power law parameters, too. This is the reason why all the CRF energies listed in Table I were obtained from Eq. 7.

In order to better characterize CRFs we added a further step to the Crab ratio described in the previous section. Indeed, by multiplying the ratio by a $E^{-2.1}$ power law (the functional form of the Crab nebula spectrum), and dividing by the functional describing the continuum shape of the source, any feature above the continuum will be greatly enhanced. This procedure (that we call Normalized Crab Ratio — NCR) has been successfully applied to the X-ray binary pulsars listed in Table I and the result is shown in Fig. 2 for some of them.

From this figure it is evident that the higher the CRF energy, the wider the feature. This is easily understood in terms of Doppler broadening of the electrons responsible of the resonance, and holds for all the sources displaying single CRFs (Orlandini & Dal Fiume 2001). In other words, it seems that the temperature of the electrons responsible of CRFs is the same for all X-ray binary pulsars, and is in the range ~ 15 – 30 keV. This energy range is somehow “critical”, as pointed out before (see also Coburn et al. 2002 for RXTE results), because it is the range in which the spectrum of X-ray pulsars shows a change of slope. On the other hand, the same relation found for the fundamental does not hold for higher CRF harmonics: this means that the temperature of the electrons responsible of higher CRF harmonics is different from that of the electrons responsible of the fundamental CRF. It is also worth noting that the Vela X-1 NCR does not show any CRF at ~ 25 keV.

4. Conclusions

The study of X-ray binary pulsars, especially in the hard X-ray band, received a new momentum from the results by BeppoSAX and RXTE. Besides the direct measurement of the neutron star magnetic field strength, the observation of CRFs can give hints on the physical processes occurring in extreme condition of temperature, density, gravity and magnetic field. It will be up to new missions (INTEGRAL, AGILE, ASTRO-E2) to find the answers to the issues that were raised by their predecessors.

References

- Arons, J., & Lea, S.M. 1976, ApJ 207, 914
 Basko, M.M., & Sunyaev, R.A. 1976, MNRAS 175, 395
 Bondi, H., & Hoyle, F. 1944, MNRAS 104, 273
 Coburn, W., Heindl, W.A., et al. 2002, ApJ 580, 394
 Cusumano, G., Di Salvo, T., et al. 1998, A&A 338, L79

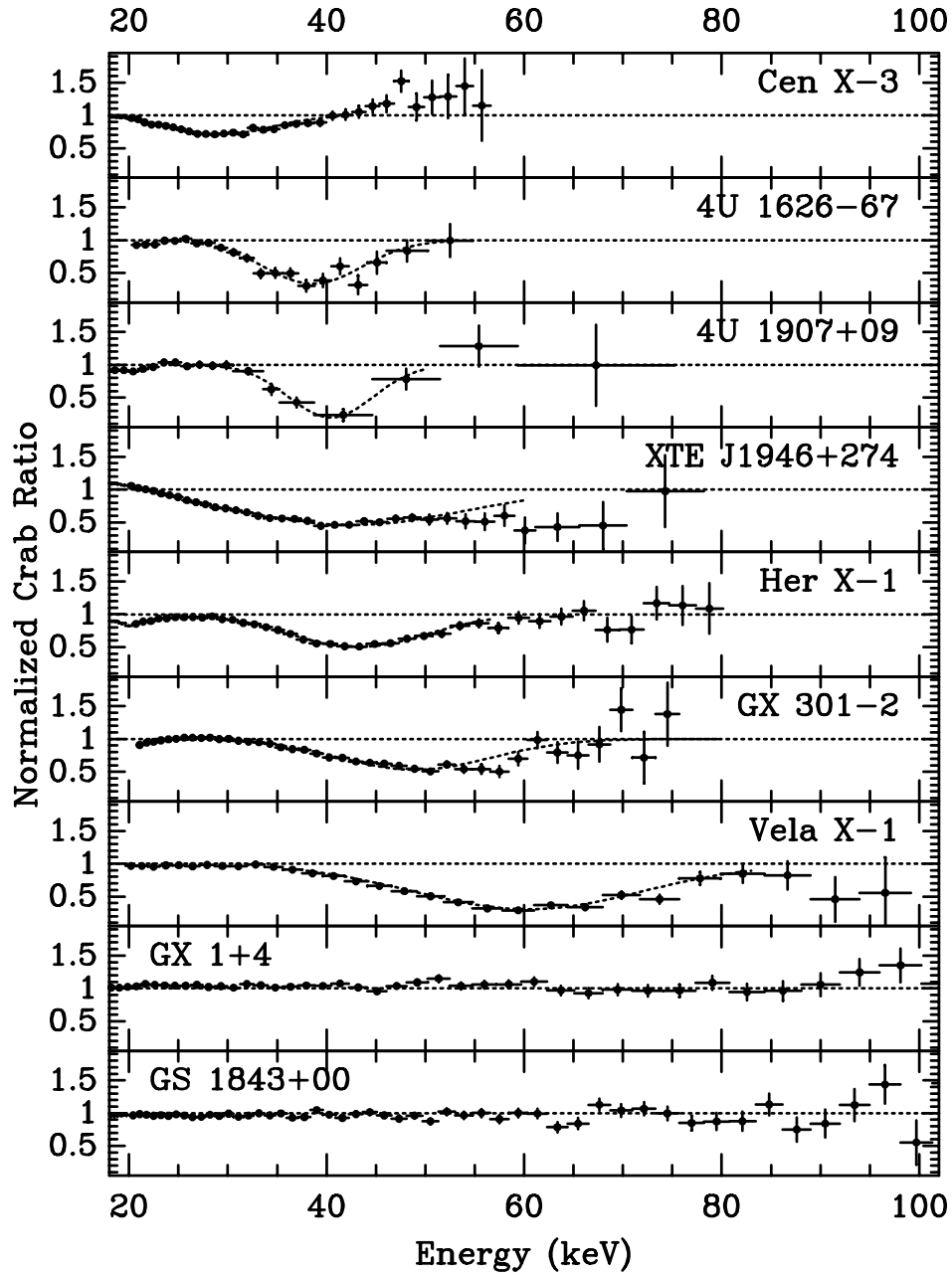


Fig. 2. Normalized Crab Ratio computed on some of the X-ray pulsars listed in Table I. Note that the higher the CRF energy, the wider the feature. For GX1+4 and GS1843+00 no CRFs are present up to 100 keV, while it is worth noting that the Vela X-1 NCR does not show any CRF at ~ 25 keV.

- Dal Fiume, D., Orlandini, et al. 1998, A&A 329, L41
 Di Salvo, T., Burderi, L., et al. 1998, ApJ 509, 897
 Elsner, R.F., & Lamb, F.K. 1977, ApJ 215, 897
 Frank, J., King, A.R., & Raine, D.J. 1985, *Accretion Processes in Astrophysics*, Cambridge University Press
 Giacconi, R., Gursky, H., et al. 1971, ApJ 167, L67
 Giacconi, R., Gursky, H., et al. 1962, Phys. Rev. Lett. 9, 439
 Ginzburg, V.L. 1970, *The Propagation of Electromagnetic Waves in Plasmas*, Pergamon Press
 Harding, A.K. 2003, in Pulsars, AXPs and SGRs observed with BeppoSAX and other Observatories, eds. Cusumano, G., Massaro, E., & Mineo, T., Aracne Editrice, p. 127
 Herold, H. 1979, Phys. Rev. D19, 2868
 Illarionov, A.F., & Sunyaev, R.A. 1975, A&A 39, 185
 Israel, G.L., Angelini, L., et al. 1998, Nucl. Phys. B 69, 141
 Kreykenbohm, I., Coburn, W., et al. 2002, A&A 395, 129
 La Barbera, A., Santangelo, A., et al. 2003, A&A 400, 993
 Makishima, K., & Mihara, T. 1992, in Frontiers of X-ray Astronomy, eds. Tanaka, Y., & Koyama, K., Universal Academy Press, p. 23
 Mereghetti, S., Chiarlone, L., et al. 2002, in Neutron Stars, Pulsars and Supernova Remnants, eds. Becker, W., Lesh, H., & Trümper, J., MPE-Report 278, p. 29
 Mészáros, P. 1992, *High-Energy Radiation from Magnetized Neutron Stars*, Chicago University Press
 Mihara, T. 1995, PhD Thesis, RIKEN, IPCR CR-76
 Orlandini, M., Bartolini, C., et al. 2004, in Proc. of the II BeppoSAX Meeting: The Restless High-Energy Universe, eds. van den Heuvel E.P.J., in 't Zand J.J.M., & Wijers, R.A.M.J., Elsevier, to appear (astro-ph/0309819)
 Orlandini, M., & Dal Fiume, D. 2001, in X-ray Astronomy '99, eds. White, N.E., Malaguti, G., & Palumbo, G.G.C., AIP Conference Series Vol. 599, p. 283
 Orlandini, M., Dal Fiume, D., et al. 1998a, A&A 332, 121
 Orlandini, M., Dal Fiume, D., et al. 1998b, ApJ 500, L163
 Orlandini, M., Dal Fiume, D., et al. 1999, A&A 349, L9
 Orlandini, M., Dal Fiume, D., et al. 2000, ASR 25, 417
 Piraino, S., Santangelo, A., et al. 2000, A&A 357, 501
 Prendergast, K.H., & Burbidge, G.R. 1968, ApJ 151, L83
 Robba, N.R., Burderi, L., et al. 2001, ApJ 562, 950
 Rybicki, G.B., & Lightman, A.P. 1975, *Radiative Processes in Astrophysics*, John Wiley & Sons
 Sandage, A., Osmer, P., et al. 1966, ApJ 146, 316
 Santangelo, A., Del Sordo, S., et al. 1998, A&A 340, L55
 Santangelo, A., Segreto, A., et al. 1999, ApJ 523, L85
 Schreier, E., Levinson, R., et al. 1972, ApJ 172, L79
 Shapiro, S.L., & Teukolsky, S.A. 1983, *Black Holes, White Dwarfs and Neutron Stars. The Physics of Compact Objects*, John Wiley & Sons
 Shklovskii, I.S. 1967, ApJ 148, L1
 Sunyaev, R.A., & Titarchuk, L.G. 1980, A&A 86, 121
 Tanaka, Y. 1986, in Radiation Hydrodynamics in Stars and Compact Objects, eds. Mihalas, D., & Winkler, K.H., Springer, p. 198
 Tananbaum, H., Gursky, H., et al. 1972, ApJ 174, L143
 Thompson, C., & Duncan, R.C. 1995, MNRAS 275, 255
 Thompson, C., & Duncan, R.C. 1996, ApJ 473, 322
 Trümper, J., Pietsch, W., et al. 1978, ApJ 219, L105
 Wheaton, W.A., Doty, J.P., et al. 1979, Nat 282, 240
 White, N.E., Swank, J.H., & Holt, S.S. 1983, ApJ 270, 711